Tracking magma spine extrusion and Deformation detection of Shiveluch volcano, Kamchatka in October 2020

Saurav Bhatta

816198

bhatta@uni-potsdam.de

ABSTRACT

Shiveluch volcano is an active volcano and the current active period started around 900 BC: since then, the large and moderate eruptions has been following each other in 50–400 years-long intervals. However, the modern eruption period began in August 1999 and has more recently consisted of ongoing explosions, frequent ash emissions, incandescent block avalanches, and lava dome growth. Lava spines are formed on top of the summit due to the slow extrusion of the lava. These spines can reach heights anywhere from 40 to 300 m tall and generally can collapse under the influence of its own weight when they grow beyond 100 meters. This could cause pyroclastic density currents that directly affect the areas around it. So, continuous monitoring and disaster response to hazards of volcanic activity are crucial. In this study, the summit spine of the Shiveluch volcano was analyzed using high-resolution Pleiades satellite pictures and planet labs photographs. Deformation using Sentinel-1A images was also examined using SNAP. Displacements was analyzed using PIV on two sets of data collected 12 days apart in ImageJ, and all the suitable data for the month of October 2020 for both ascending and descending pathways was examined for deformation.

Keywords: Shiveluch volcano, Spine, Magma extrusion, PIV, InSAR, Displacement map

1. INTRODUCTION

Kamchatka, an eastern Russian peninsula, borders the Sea of Okhotsk, Pacific Ocean, and Bering Sea. At its broadest, it stretches 1,200 km north-south and 480 km east-west. Sredinny ("Central") and Vostochny ("Eastern") mountain ranges reach 4,750 meters in Klyuchevskaya Volcano along the peninsula. The Kamchatka River dominates the valley between these mountain ranges, which has 22 active volcanoes, geothermal, and hot springs out of 127 total.(Kamchatka Peninsula | Location, Climate, Volcanoes, & Facts | Britannica, n.d.). Shiveluch is one of the largest, most active, and longest-erupting volcanos on the Kamchatka Peninsula and is one of the most active volcanoes in the world. About 0.015 km³ of magma is produced each year in Shiveluch, leading to explosive avalanches and lava domes (V et al., 2007; Heap et al., 2016). Within the scarp formed by the great south-flank collapse after the Plinian explosion of 1964, the "Young Shiveluch" dome first appeared in 1980. Since then, the dome has formed and collapsed several times, resulting in multiple ash clouds, pyroclastic flows, block-and-ash flows, and even two "whaleback domes"(Global Volcanism Program | Report on Sheveluch (Russia) — July 2022, n.d.).

Lava spines are outcrops of magma that come from volcanoes. They give researchers a rare look at how the conduit and shear processes work (Walter et al., 2022). Most of the time, extrusion is slow and has to do with the release of gases before an eruption and the solidification of the melt. Depending on the rheology and the rate of extrusion, lava spines can grow to be anywhere from 40 to 300 m tall. This has been seen in mountains all over the world. But nevertheless, when spines reach heights of more than 100 meters, they often collapse from their own weight. This could cause pyroclastic density currents that directly affect the areas around it. (Walter et al., 2022). Magma extrusion rate and rheology of magma may greatly influence spine geometry, where Low extrusion rates (below ~1 m³/s) allow greater time for outgassing and crystallization, forming vertical spines. This makes the magma to solidify and harden, enabling tall vertical structures. (Heap et al., 2016 cited according to Walter et al., 2022) Thus, it is crucial for risk assessment and early warning systems to have a knowledge of the directional cues of spine growth and breakdown. (Walter et al., 2022)

Therefore, in this work, we are using the images from planet lab and high-resolution images from Pleiades satellite to study magma spine extrusion and deformation detection over a short period of time. Planet Labs is a network of hundreds of low-cost satellites captures high-resolution Earth imagery every day. Traditional satellite imagery suppliers use fewer large, expensive satellites. Planet Labs data is affordable, high-temporal frequency, global, and high-resolution (3-meters). Changes on the ground may be tracked in near real time because to Planet Labs' daily imaging capabilities. This has a wide range of potential uses, from monitoring infrastructure and land usage to responding to natural disasters (Planet Team, 2017).

With its high activity and constant deformation, Shiveluch volcano should be closely monitored, ideally on a daily basis. Having high-quality, frequent data allows for better disaster response and lowers the impact of volcanic hazards. In our case we are using planet labs data to scale the ortho-images created from Pleiades satellite. The French space agency CNES operates the high-resolution Pleiades satellites for Earth monitoring. This satellite can take panchromatic photos with a ground resolution of 30 centimeters and multispectral images with 70 centimeters (*Pléiades | Very High-Resolution (50cm) Satellites*, n.d.).

Therefore, with this study, we are using planet labs, Pleiades satellite and sentinel-1 images. we would like to know the particle image velocimetry (PIV) from (i.e., 01-oct-2020 – 13-oct-2020) and deformation from (4 scenes from oct-2020(07, 13, 19, 25) of Shiveluch volcano using a displacement maps and interpret the results.

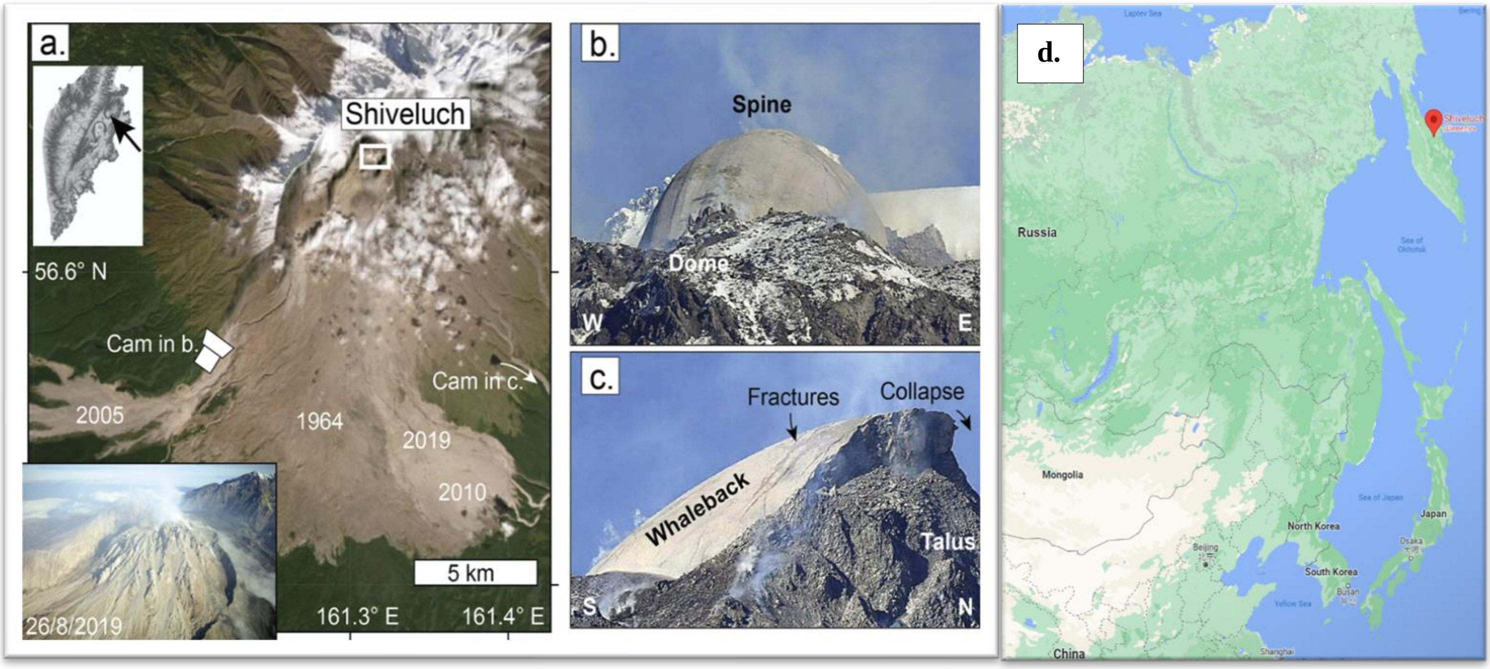

Figure 1. **(a.)** Satellite image shown in top left and helicopter image on bottom left shown. The years indicated on the figure represents the pyroclastic density current deposits (2005, 2010, 2019) & debris avalanche (1964). **(b, c)** Photos showing the whaleback spine taken on 28.09.2020 from the cam locations as illustrated in figure a. See the steep slope and fractures in fig c. **(d.)** Picture showing the location of the Shiveluch volcano on a world map view in google maps. (Walter et al., 2022)

2. METHODS

2.1 Data acquisition for Particle Image Velocimetry (PIV)

In this study, we will study the alterations in the spine, especially the structure of the whaleback spine at the peak of the Shiveluch volcano. We will conduct a PIV analysis for the two images acquired by the high-resolution imaging satellite Pleiades on October 1, 2020 and October 13, 2020, respectively. Prof. Walter provided high-resolution satellite imagery for both aforementioned days. As both pictures were photographs, they must be orthorectified before further analysis can be conducted. Thus, Professor Walter also provided georeferenced images from planet labs satellites at the same time. These georeferenced photos may be utilized to orthorectify the high-quality Pleiades satellite imagery. Hence, all of Prof. Walter's images, including two high-resolution images from the Pleiades satellite and georeferenced images from planet labs, were utilized for PIV analysis.

2.1.1 Particle Image Velocimetry (PIV) process

Particle Image Velocimetry (PIV) is an optical measurement method in which the velocity field of an entire flow region is measured in one measurement. (Atkins, 2016). With the process of cross-correlating sets of two images and gradually shrinking the window size, it is possible to improve the PIV resolution. As mentioned above, the georeferenced images from planet labs satellites were used to orthorectify the two high-resolution images from Pleiades satellite. ImageJ 1.53t version was used for the further analysis. MtrackJ and PIV plugins were used within ImageJ. The images were stacked into ImageJ and then cropped to the area of interest. For MtrackJ, two stacked images were carefully marked and saved to track the movement. Likewise for PIV, Iterative PIV (Cross-Correlation) plugin was used, with window sizes of 128, 64, and 32 for PIV1, PIV2, and PIV3, respectively; normalized median test and invalid findings were changed for median with noise and threshold for normalized median test, set to 0.5 and 5, respectively. Subsequently, a vector plot was made using PIV's plot tool based on the final result (figure 15).

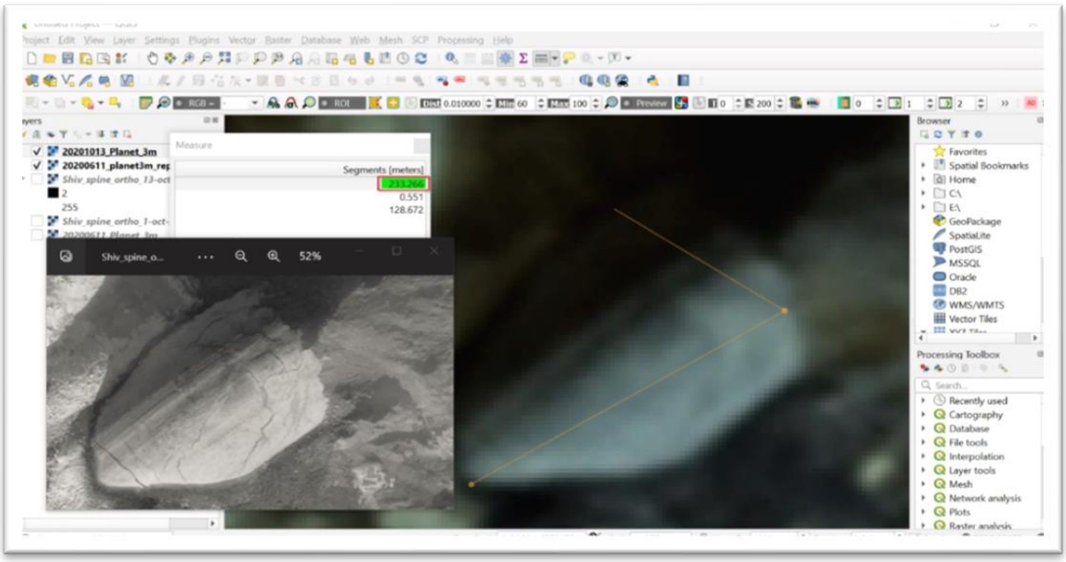

Figure 2. Measuring the length on QGIS from the planet labs Geo tiff data.

Figure 3. Updating the pixel length to the known measurement in meters in ImageJ.

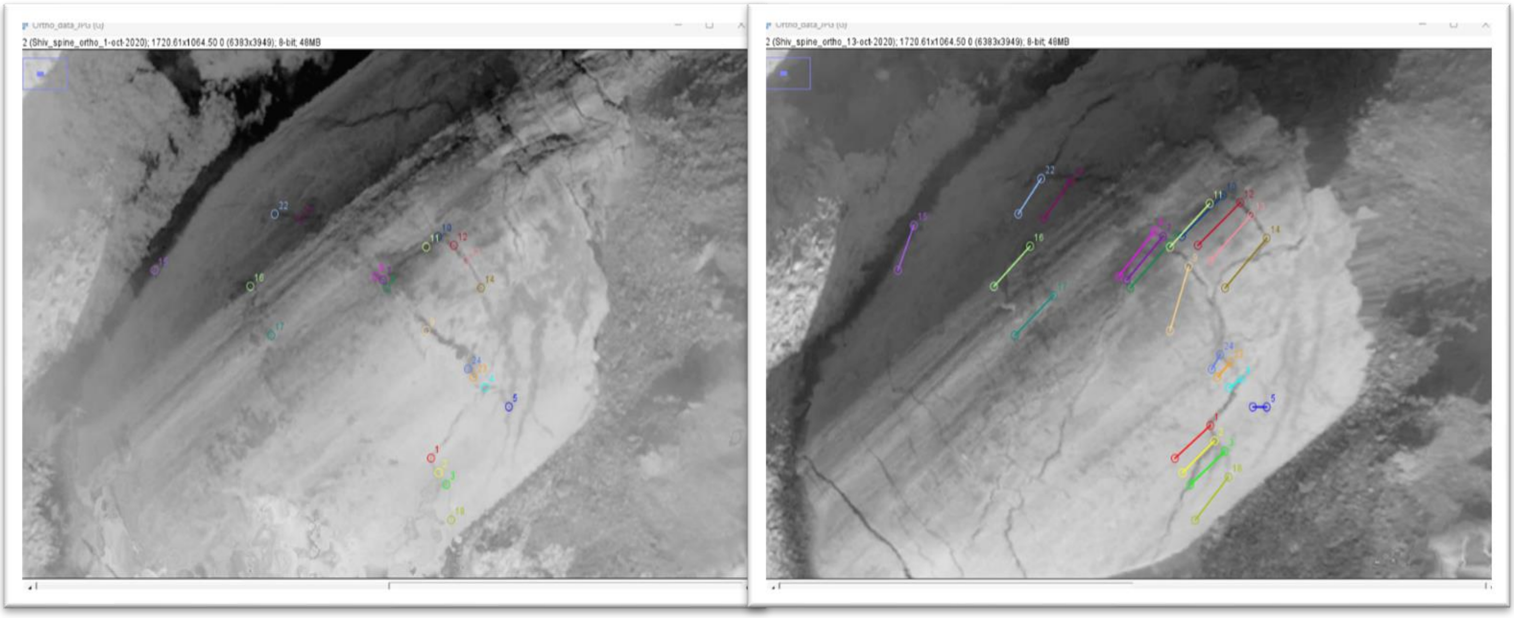

Figure 4. Location of the 22 reference points(01-oct-2020) (left) and their respective displacement (13-oct-2020) (Right) of the two high resolution ortho-images from Pleiades satellite.

Table 1. Displacement results in meters from MtrackJ: Points data.

				MTrackJ: Points data							
Points no.	**1**	**2**	**3**	**4**	**5**	**6**	**7**	**8**	**9**	**10**	11
MTrackJ results (Displacement) (m)	17.766	16.432	17.602	5.583	5.394	20.417	20.208	21.636	22.632	20.934	21.263
Points no.	**12**	**13**	**14**	**15**	**16**	**17**	**18**	**19**	**20**	**21**	**22**
MTrackJ results (Displacement) (m)	21.724	22.179	23.193	16.285	19.381	20.11	19.342	16.728	14.88	6.862	6.081

2.2 Data acquisition for Interferometric synthetic aperture radar (InSAR)

Information about Earth's surface may be obtained using interferometric synthetic aperture radar (InSAR), which does so by emphasizing on the phase difference between two complicated radar SAR scans obtained from slightly different sensing positions. Because it uses microwaves, it can see through clouds, and since it's an active system, it can work both day and night.

A digital SAR image can be thought of as a mosaic, which is a two-dimensional grid made up of small picture pieces (pixels). Each pixel represents a small area of the Earth's surface. This small area is called a "resolution cell." Using complex numbers, the resolution cell conveys two pieces of information: amplitude and phase. The amplitude depends on how rough the surface is, so it is high in cities and on rocky cliffs and low on smooth, flat surfaces like the quiet ocean surface. Likewise, the amplitude of SAR picture is shown as a range of grayscale values, with brighter pixels indicating more backscattered radiation and darker pixels indicating less. However, Phase is mostly information on the distance between the targets on the ground and the satellite antenna.
An interferogram is created by measuring the interference pattern of two or more waves. This processs is achiecved by the coregistration step, in which two or more synthetic aperture radar (SAR) images of the same place are aligned precisely on a subpixel level. (Braun & Veci, 2021; Ferretti et al., 2007)

Four Sentinel-1A scenes (Fig.5), two ascending and two descending, were downloaded from the Alaska Satellite Facility for the Shiveluch volcano on different dates in October 2020. SNAP (version 9.0.0), which is the European space agency's (ESA) free, open-source satellite imagery processing and Earth observation platform, was used to perform additional analysis on the data that had been downloaded.

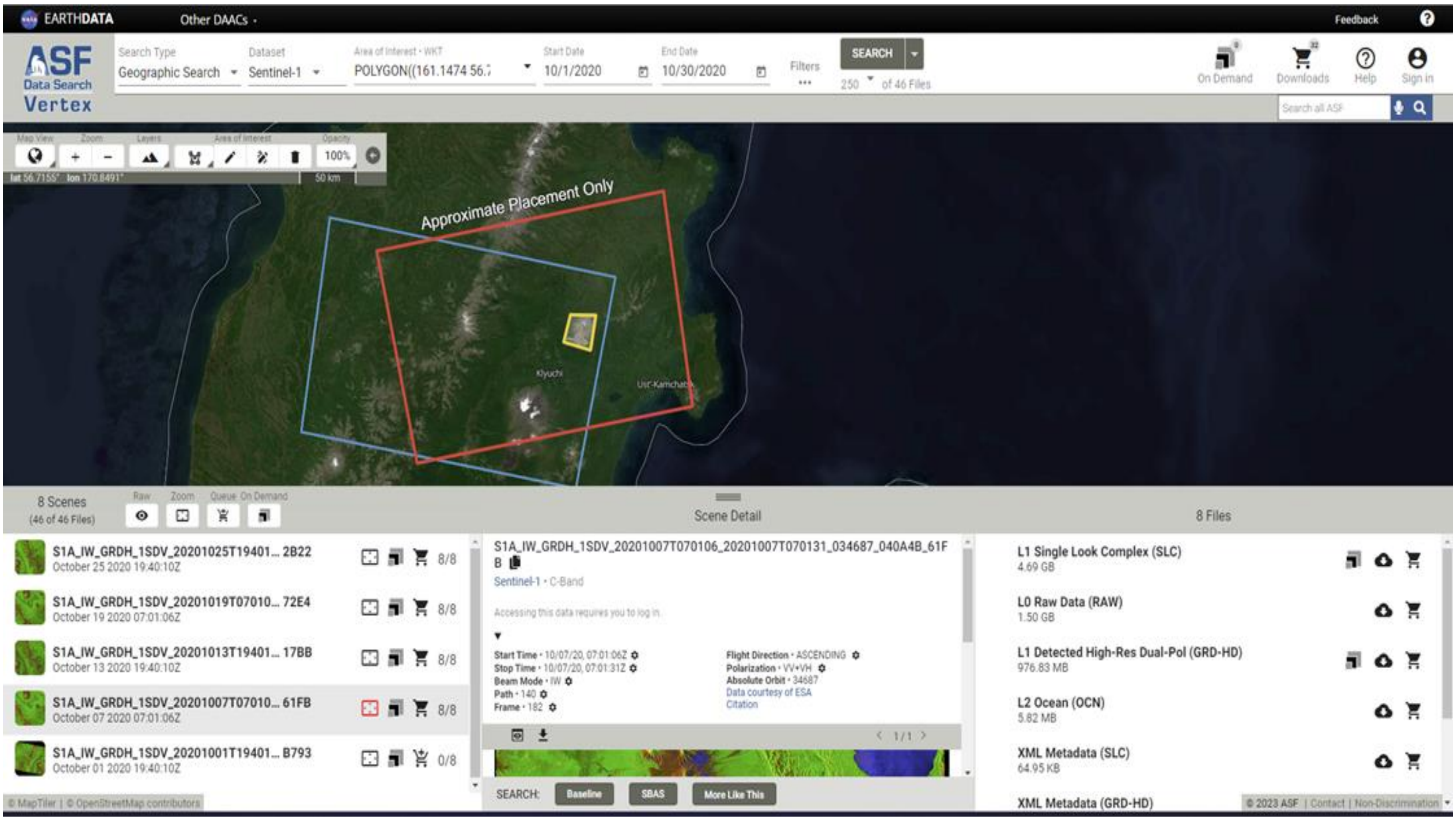

Figure 5. Selected 4 scenes in total (2 ascending, 2 descending)

2.2.1 Interferometry (InSAR) process

The Interferometry process was performed in a step-by-step process as shown in Figure 8 & 7, which was developed by the graph builder inside SNAP software. All the downloaded scenes were imported to the SNAP product explorer. TOPSAR-Split was performed as it only selects the bursts that are needed for the analysis. As a next step Apply-orbit-file was performed, it corrects for any errors in the satellite's position and velocity during the data acquisition. The produced image after this step is then co-registered using the Back-geocoding function. The image produced after this step is already a interferogram, but no valuable information can be achieved from this as it is still in radar coordinate system. Hence, to get any valuable information out of it, it needs to be converted into geographic coordinate system. Therefore, SRTM 3sec as a DEM was used to coregister the obtained images and the phase and coherence band was generated as seen in figure 9. Then, using the interferogram tool and a coherence range window size of 20, the interferogram was created. Following that, the image was then processed to get rid of the black lines between the bursts using the TOPSAR-Deburst tool, and finally, it was exported.

The exported image is then again processed further using the Topo phase removal tool, this step is used to correct the effect of topography on the interferometric phase. This tool initially creates a DEM of the study area using radar interferometry or other high-resolution data sources. The DEM simulates radar wave propagation and estimates topography-induced phase contribution. Removing this phase input from the interferogram improves surface deformation measurement. In our case SRTM 3Sec for the digital elevation model was used.
The next step in processing is multilook, which is done to increase the interferogram's signal-to-noise ratio (SNR) and decrease the data's spatial resolution. Our work here used Multilook, with 8 range looks, to transform the original lengthy strip into square pixels with a mean ground square pixel size of roughly 30. Goldstein Phase Filtering tool is used after this step. This tool is used to filter the interferometric phase data and get rid of noise and other unwanted shifts. The phase unwrapping steps is then performed after this step.

Figure 6. Detailed steps for Interferogram process in SNAP.

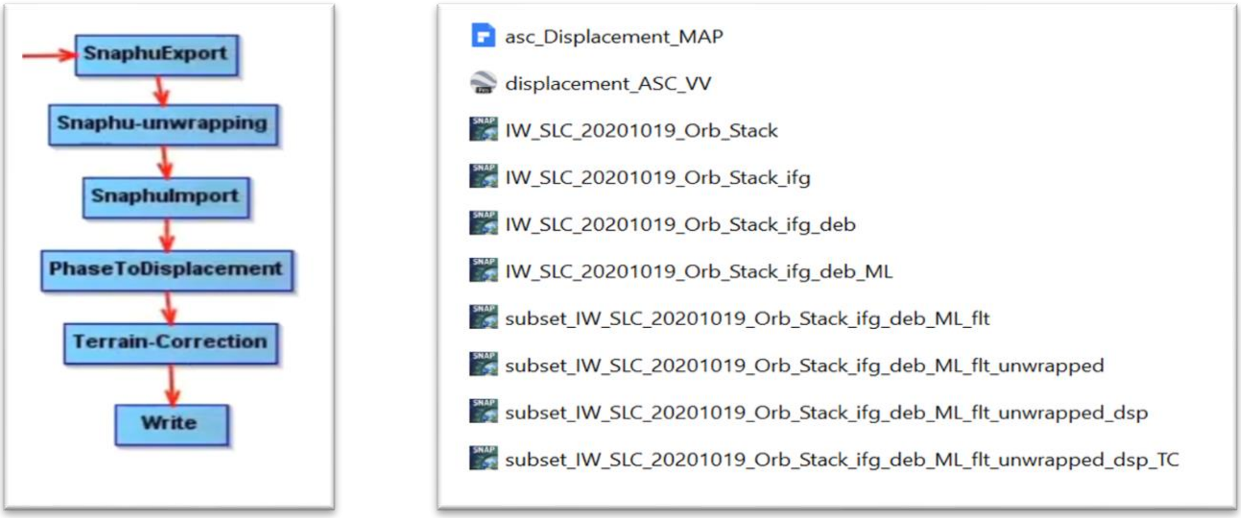

Figure 7. SNAPHU steps (left), file's structure overview after each step of InSAR processing (right).

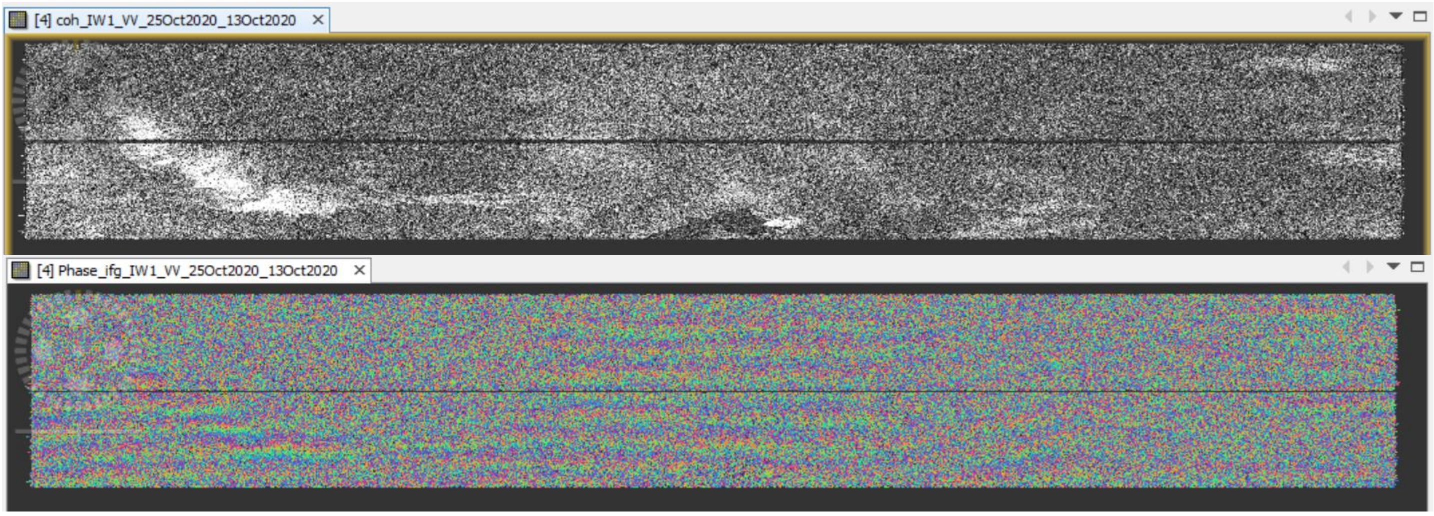

Figure 8. Coherence(top) and Phase band of the Area of interest (Shiveluch Mountain).

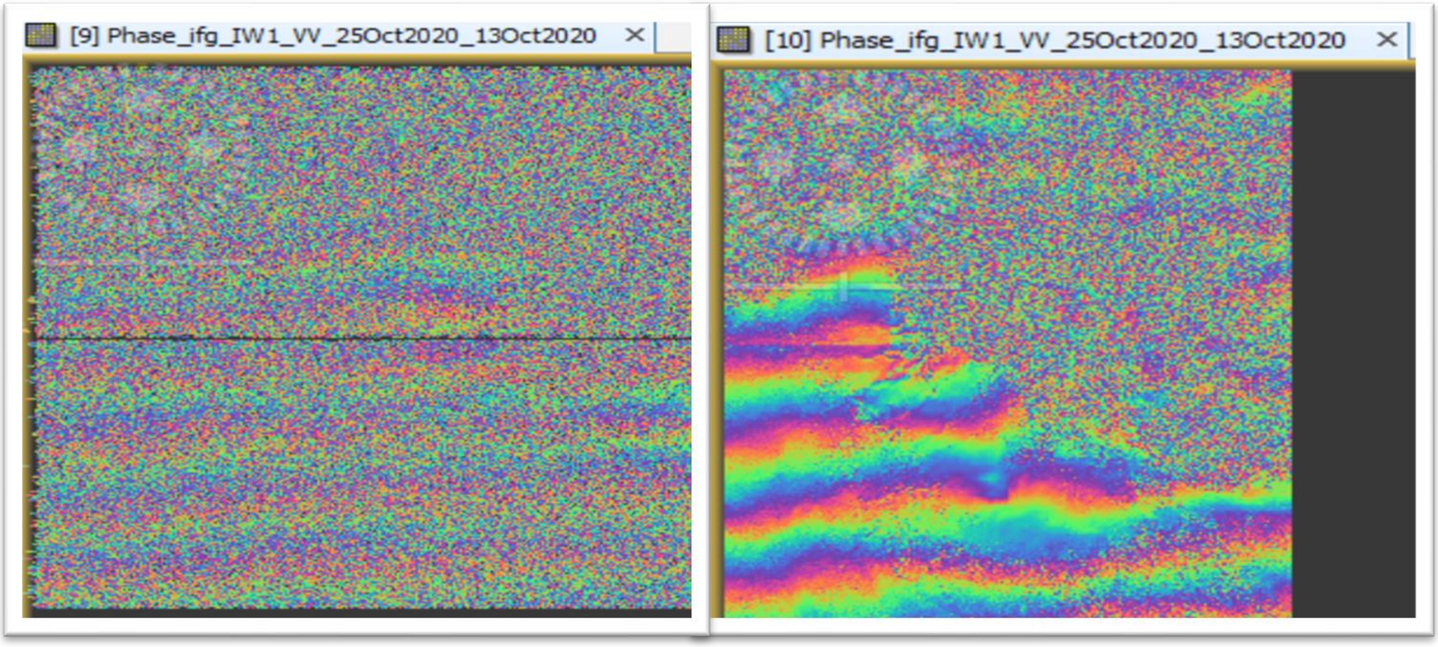

Figure 9. Interferogram before (left) and after (right) Goldstein Phase filtering for descending scene of AOI. The horizontal lines even after TOPSAR-Deburst was not removed for unknown reasons.

2.2.2 Phase Unwrapping

The process of phase unwrapping is used to compensate for phase ambiguities that occur during interferometric phase measurement. During the InSAR processing, the interferometric phase data is measured as a continuous value. However, because of the way the radar wave works, the phase can only be measured within a certain range, called the "wrapped" phase. This means that the phase values that are measured are the phase's remainder divided by 2π. Because of this, the phase values can be confusing and look like they abruptly cease and resume. This makes it hard to understand the data and find the real surface deformation signal.(Braun & Veci, 2021).

In SNAP, the unwrapping process consisted of three stages: exporting the data, unwrapping it, and importing it.

For exporting the data, DEFO as a Statistical-cost mode was selected and MCF as an Initial method was selected from the drop-down menu as the parameters for the process. The Run tab is then selected, this process than creates number of files in a project folder. One of the generated files named 'Phase.hdr' was selected for unwrapping step as I/O Parameters. Following all this processing, we exported the unwrapped phase interferogram shown in figure 11 using Snaphu's import tool.

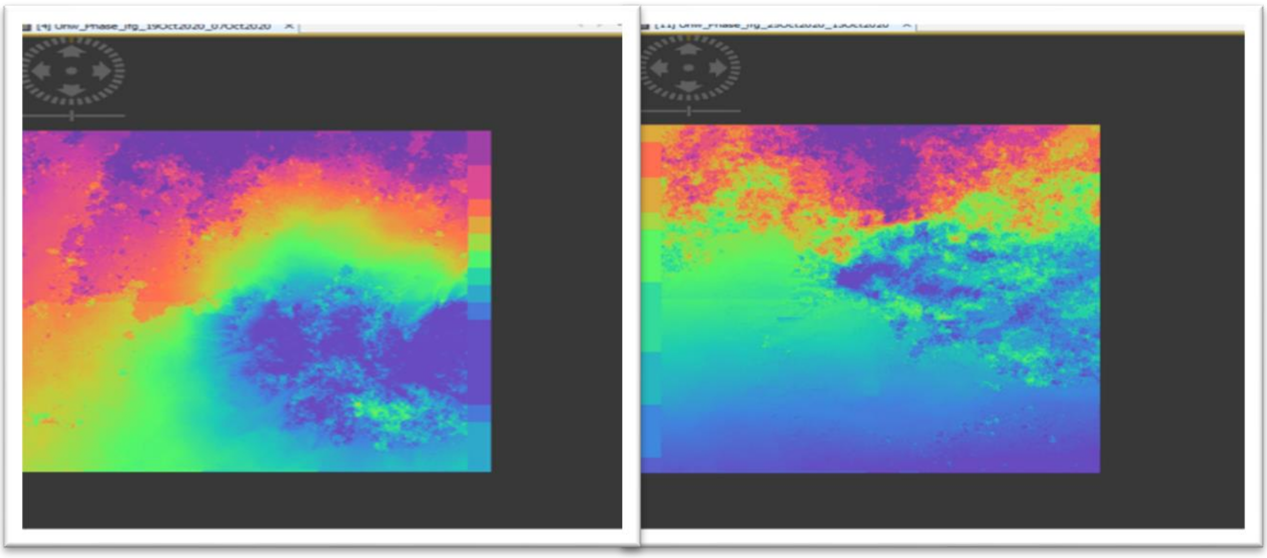

Figure 10. Unwrapped phase of interferometry in SNAP, Ascending (left) & Descending (Right)

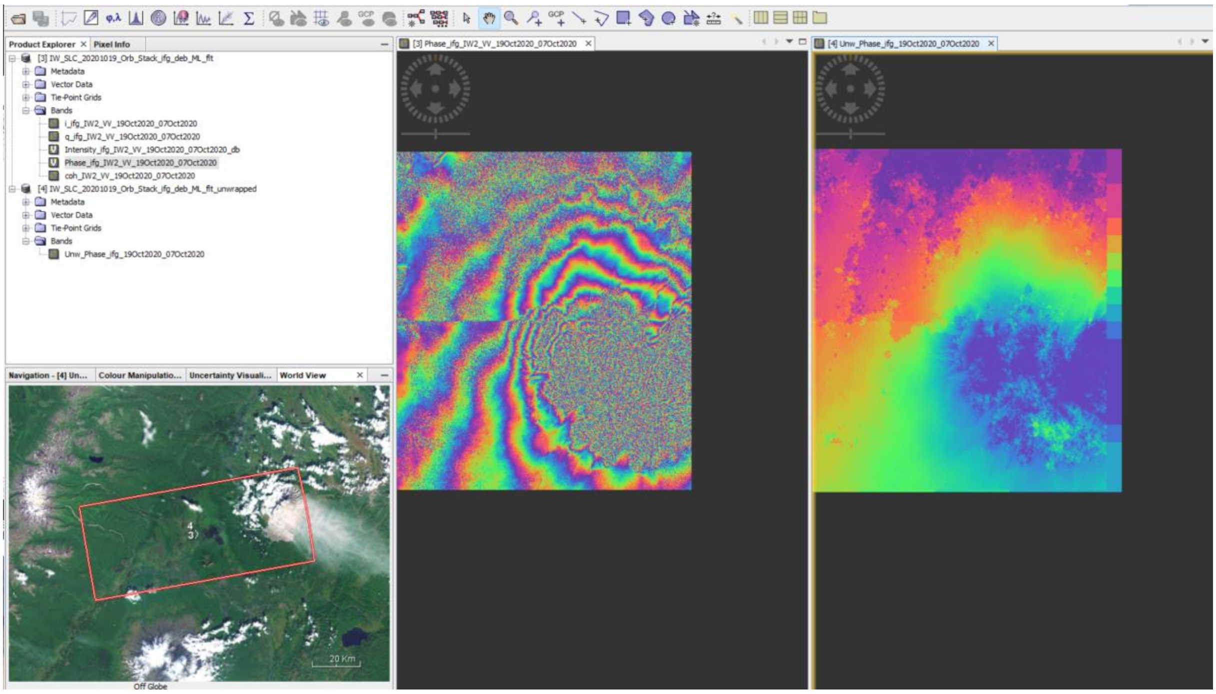

Figure 11. Interferogram after Goldstein phase filtering (left) and unwrapped phase after SNAPHU import (Right) for ascending scene.

2.2.3 Phase to Displacement

Proceeding from the previous step, the displacement map was created after completing the phase unwrapping step using phase to displacement tool. The step was followed according to chronology shown in figure.7. The produced displacement map was then utilized to do terrain correction using the Doppler Terrain correction tool as the subsequent step.

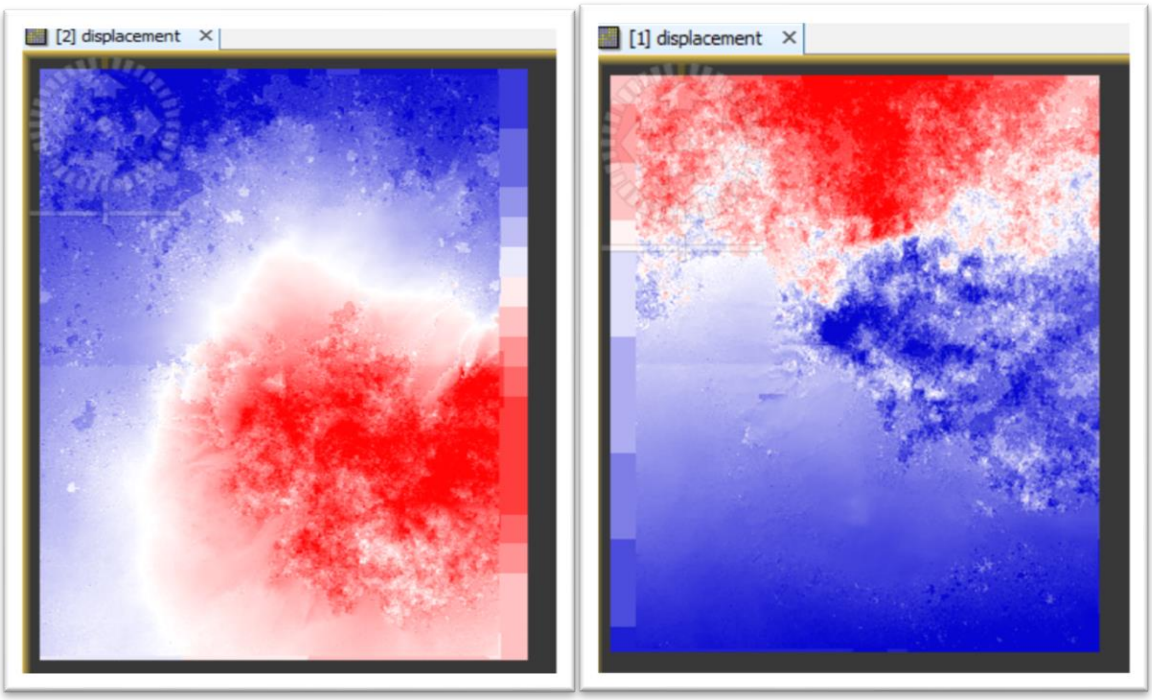

Figure 12. Displacement map for Ascending (left) and Descending (Right) from unwrapped phase interferometry of cropped AOI.

3. RESULTS AND DISCUSSIONS

3.1 Particle Image Velocimetry (PIV) analysis

The figure below displays the masked image (left) and the corresponding PIV vector graph (right). The precise placement of the two figures on top of one another might be tricky. Nevertheless, direct examination reveals displacements in the top-right and bottom-center regions, where mostly green to red vector arrows are visible. Two high-resolution images were evaluated: one from October 1, 2020, and another from October 13, 2020. From the vector graph, we can see that the maximum distance the object migrated was 87 pixels.

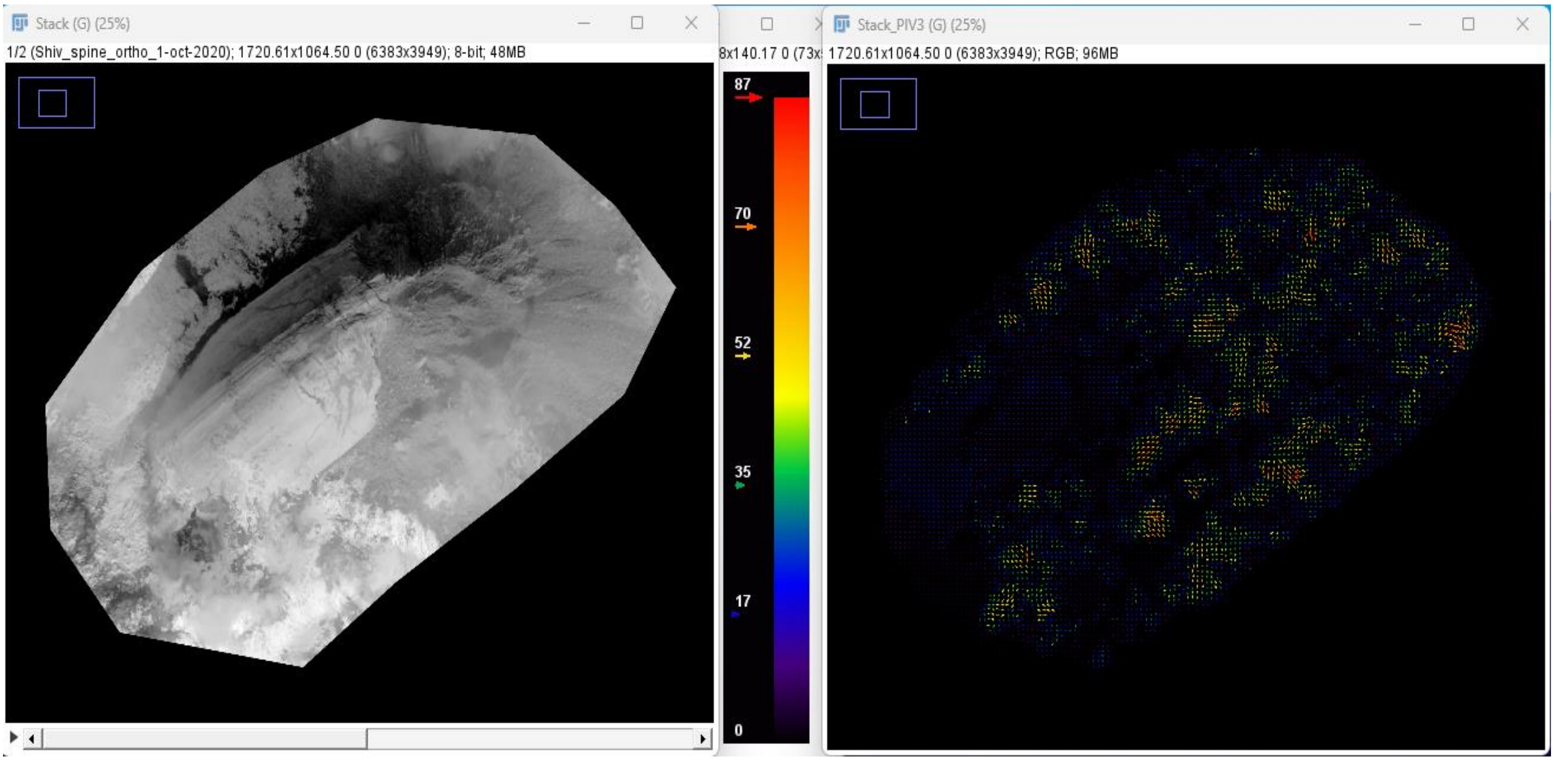

Figure 13. Comparing the masked image (Left) and the PIV vector graph (Right)generated from PIV plugin to evaluate the results.

3.2 Displacement map

Based on the data collected for both orbits going up and orbits going down, the phase unwrapping steps were done for both. Figure 13 and 14 shows ascending and descending displacement maps made from these unwrapped interferograms respectively. The area where the distance between the satellite and the ground has risen is shown in blue, and the contrary is shown in yellow. Where a decrease in distance means "uplift" and an increase in distance means "subsidence." Therefore, area in blue is subsiding and the area towards yellowish color bar is uplifting.

Hence, based on results, in ascending scene displacement map, there is maximum subsidence of 25.5 cm and uplift of 6.1 cm. Similarly, in descending scene of displacement map, there is a maximum subsidence of 18 cm and an uplift of 11 cm.

In both ascending and descending displacement maps, deformation can be observed near the summit area. However higher level of deformation can be seen in ascending scene than in descending scene. Different date of data acquisitions for both ascending and descending scenes could be an explanation on the difference. Likewise, some uplift can also be observed outside the area of interest.

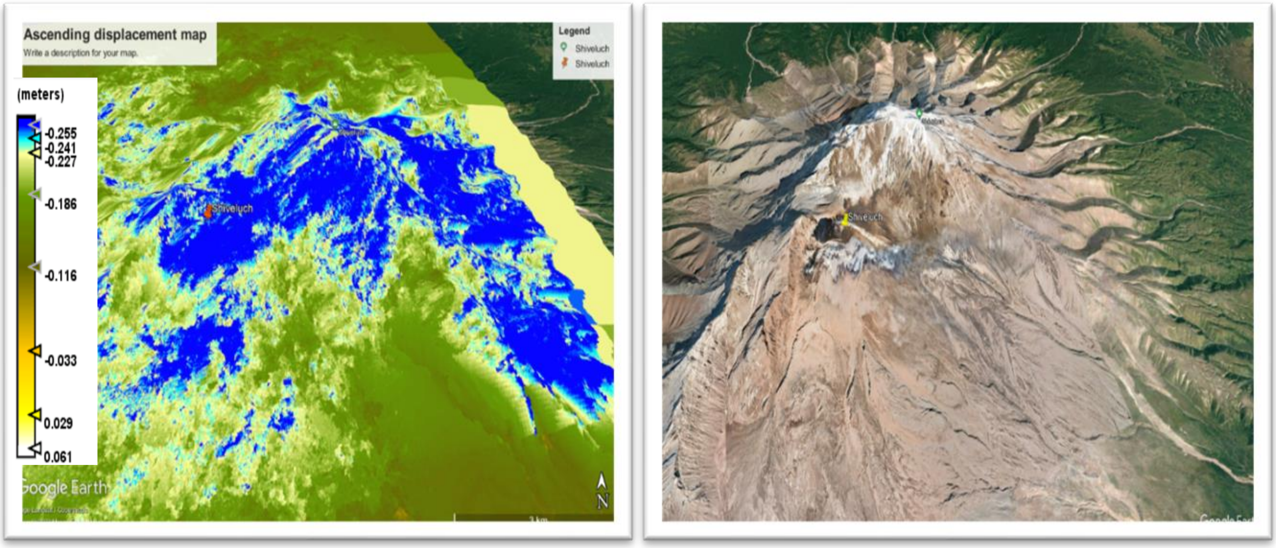

Figure 14. Ascending displacement map (Left) and the respective google earth view of Area of Interest (Right).

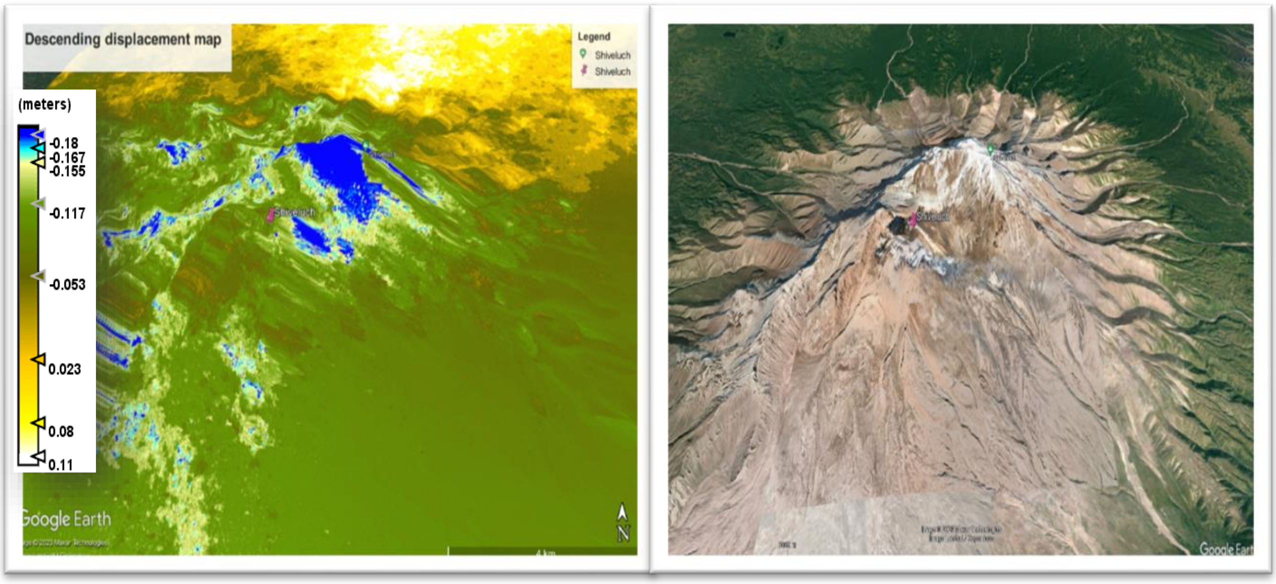

Figure 15. Descending displacement map (Left) and the respective google earth view of Area of Interest (Right).

4. CONCLUSION

The manual tracking and PIV analysis clearly indicates the displacements on the summit area where whaleback spine structure is located on Shiveluch volcano. The growing spine is ultimately collapsing after a certain threshold. This can create pyroclastic density currents that directly affect the areas around it. Likewise, from the displacement maps created from InSAR processing steps, for both ascending and descending maps, the subsidence is indicated near summit area of the Shiveluch volcano. Shiveluch's near-constant eruptive activity makes it a top priority for North Pacific hazard monitoring (Ramsey et al., 2012). In settlements within several hundred kilometers of the volcano, ash-fall can affect daily life. Furthermore, drifting ash clouds often cross the Bering Sea and Pacific Ocean onto international passenger and freight aviation routes. As both PIV and InSAR analysis methods point to deformation near the summit area. I would advise the local government to notify people for the caution and more importantly notification to the aviation authority about the potential hazardous situation due to ash clouds.

REFERENCES

Atkins, M. D. (2016). Chapter 5—Velocity Field Measurement Using Particle Image Velocimetry (PIV). In T. Kim, T. J. Lu, & S. J. Song (Eds.), *Application of Thermo-Fluidic Measurement Techniques* (pp. 125–166). Butterworth-Heinemann. https://doi.org/10.1016/B978-0-12-809731-1.00005-8

Braun, A., & Veci, L. (2021). TOPS Interferometry Tutorial. *Sentinel-1 Toolbox*.

Ferretti, A., Monti-Guarnieri, A., Prati, C., Rocca, F., & Massonet, D. (2007). InSAR Principles—Guidelines for SAR Interferometry Processing and Interpretation. *ESA Training Manual*, *19*.

Global Volcanism Program | Report on Sheveluch (Russia)—July 2022. (n.d.). Retrieved 11 March 2023, from https://volcano.si.edu/ShowReport.cfm?doi=10.5479/si.GVP.BGVN202207-300270

Heap, M. J., Russell, J. K., & Kennedy, L. A. (2016). Mechanical behaviour of dacite from Mount St. Helens (USA): A link between porosity and lava dome extrusion mechanism (dome or spine)? *Journal of Volcanology and Geothermal Research*, *328*, 159–177. https://doi.org/10.1016/j.jvolgeores.2016.10.015

Kamchatka Peninsula | Location, Climate, Volcanoes, & Facts | Britannica. (n.d.). Retrieved 11 March 2023, from https://www.britannica.com/place/Kamchatka-Peninsula

Planet Team (2017). Planet Application Program Interface:In Space for Life on Earth. San Francisco, CA. Retrieved 12 March 2023, from https://www.planet.com/company/

Pléiades | Very High-Resolution (50cm) Satellites. (n.d.). Retrieved 12 March 2023, from https://www.intelligence-airbusds.com/imagery/constellation/pleiades/

Ramsey, M. S., Wessels, R. L., & Anderson, S. W. (2012). Surface textures and dynamics of the 2005 lava dome at Shiveluch volcano, Kamchatka. *GSA Bulletin*, *124*(5–6), 678–689. https://doi.org/10.1130/B30580.1

Shiveluch Volcano, Russia's Far East. (2007, September 3). [Text.Article]. NASA Earth Observatory. https://earthobservatory.nasa.gov/images/8004/shiveluch-volcano-russias-far-east

V, P., P, K., M, P., L, S., & M, H. (2007). *HOLOCENE ERUPTIVE HISTORY OF SHIVELUCH VOLCANO, KAMCHATKA PENINSULA, RUSSIA*. https://doi.org/10.1029/172GM19

Walter, T. R., Zorn, E. U., Harnett, C. E., Shevchenko, A. V., Belousov, A., Belousova, M., & Vassileva, M. S. (2022). Influence of conduit and topography complexity on spine extrusion at Shiveluch volcano, Kamchatka. *Communications Earth & Environment*, *3*(1), Article 1. https://doi.org/10.1038/s43247-022-00491-w

APPENDIX

					MTrackJ: Points data								
NR	TID	PID	X [0]	Y [0]	t [sec]	I [val]	Len [0]	D2S [0]	D2R [0]	D2P [0]	V [0/sec]	alpha [deg]	delta A [deg]
1	1	1	748.436	606.827	0	181	0	0	NA	NA	NA	NA	NA
2	1	2	762.273	595.685	0	141	17.766	17.766	NA	17.766	NA	-38.841	NA
3	2	1	751.491	611.679	0	181	0	0	NA	NA	NA	NA	NA
4	2	2	763.891	600.896	0	154	16.432	16.432	NA	16.432	NA	-41.009	NA
5	3	1	754.366	615.632	0	175	0	0	NA	NA	NA	NA	NA
6	3	2	767.844	604.311	0	169	17.602	17.602	NA	17.602	NA	-40.03	NA
7	4	1	769.641	583.105	0	162	0	0	NA	NA	NA	NA	NA
8	4	2	774.314	580.05	0	169	5.583	5.583	NA	5.583	NA	-33.179	NA
9	5	1	778.627	589.575	0	171	0	0	NA	NA	NA	NA	NA
10	5	2	784.018	589.395	0	176	5.394	5.394	NA	5.394	NA	-1.909	NA
11	6	1	726.871	545.591	0	96	0	0	NA	NA	NA	NA	NA
12	6	2	740.619	530.496	0	102	20.417	20.417	NA	20.417	NA	-47.675	NA
13	7	1	729.836	546.804	0	102	0	0	NA	NA	NA	NA	NA
14	7	2	743.853	532.248	0	86	20.208	20.208	NA	20.208	NA	-46.081	NA
15	8	1	731.184	549.5	0	102	0	0	NA	NA	NA	NA	NA
16	8	2	746.684	534.405	0	108	21.636	21.636	NA	21.636	NA	-44.243	NA
17	9	1	746.549	563.787	0	159	0	0	NA	NA	NA	NA	NA
18	9	2	753.827	542.357	0	125	22.632	22.632	NA	22.632	NA	-71.241	NA
19	10	1	751.266	532.248	0	72	0	0	NA	NA	NA	NA	NA
20	10	2	767.17	518.635	0	72	20.934	20.934	NA	20.934	NA	-40.561	NA
21	11	1	746.549	535.752	0	68	0	0	NA	NA	NA	NA	NA
22	11	2	762.049	521.196	0	67	21.263	21.263	NA	21.263	NA	-43.202	NA
23	12	1	757.421	535.303	0	121	0	0	NA	NA	NA	NA	NA
24	12	2	773.864	521.106	0	87	21.724	21.724	NA	21.724	NA	-40.807	NA
25	13	1	762.183	540.335	0	138	0	0	NA	NA	NA	NA	NA
26	13	2	778.177	524.97	0	94	22.179	22.179	NA	22.179	NA	-43.851	NA
27	14	1	767.844	549.5	0	163	0	0	NA	NA	NA	NA	NA
28	14	2	784.018	532.877	0	167	23.193	23.193	NA	23.193	NA	-45.785	NA
29	15	1	641.33	543.749	0	97	0	0	NA	NA	NA	NA	NA
30	15	2	647.44	528.654	0	90	16.285	16.285	NA	16.285	NA	-67.964	NA
31	16	1	678.53	548.961	0	63	0	0	NA	NA	NA	NA	NA
32	16	2	692.457	535.483	0	56	19.381	19.381	NA	19.381	NA	-44.061	NA
33	17	1	686.527	565.404	0	131	0	0	NA	NA	NA	NA	NA
34	17	2	701.532	552.016	0	127	20.11	20.11	NA	20.11	NA	-41.74	NA
35	18	1	756.253	627.403	0	196	0	0	NA	NA	NA	NA	NA
36	18	2	769.192	613.026	0	195	19.342	19.342	NA	19.342	NA	-48.013	NA
37	21	1	697.758	526.318	0	42	0	0	NA	NA	NA	NA	NA
38	21	2	708.361	513.379	0	46	16.728	16.728	NA	16.728	NA	-50.667	NA
39	22	1	687.875	524.7	0	57	0	0	NA	NA	NA	NA	NA
40	22	2	696.86	512.84	0	52	14.88	14.88	NA	14.88	NA	-52.853	NA
41	23	1	764.879	579.601	0	175	0	0	NA	NA	NA	NA	NA
42	23	2	769.731	574.749	0	167	6.862	6.862	NA	6.862	NA	-45	NA
43	24	1	762.723	576.905	0	180	0	0	NA	NA	NA	NA	NA
44	24	2	766.137	571.873	0	148	6.081	6.081	NA	6.081	NA	-55.84	NA